
Research Article: Methods/New Tools | Novel Tools and Methods

Application of Recombinant Rabies Virus to Xenopus Tadpole Brain

<https://doi.org/10.1523/ENEURO.0477-20.2021>

Cite as: eNeuro 2021; 10.1523/ENEURO.0477-20.2021

Received: 3 November 2020

Revised: 13 May 2021

Accepted: 31 May 2021

This Early Release article has been peer-reviewed and accepted, but has not been through the composition and copyediting processes. The final version may differ slightly in style or formatting and will contain links to any extended data.

Alerts: Sign up at www.eneuro.org/alerts to receive customized email alerts when the fully formatted version of this article is published.

Copyright © 2021 Faulkner et al.

This is an open-access article distributed under the terms of the Creative Commons Attribution 4.0 International license, which permits unrestricted use, distribution and reproduction in any medium provided that the original work is properly attributed.

1 **Title: Application of Recombinant Rabies Virus to Xenopus Tadpole Brain**

2
3 Abbreviated Title: Application of Rabies to Xenopus

4
5 Regina L. Faulkner¹, Nicholas R. Wall², Edward M. Callaway², Hollis T. Cline¹

6
7 ¹Neuroscience Department and The Dorris Neuroscience Center, The Scripps Research Institute, La Jolla CA

8 ²The Salk Institute for Biological Sciences, La Jolla, CA

9
10 Author Contributions:

11 RLF, NRW, EMC, and HTC Designed research; RLF Performed research and analyzed data; RLF and HTC
12 Wrote the paper

13
14 Correspondence should be address to Hollis T. Cline (cline@scripps.edu)

15
16 Number of Figures: 4

17 Number of Tables: 1

18 Number of Multimedia: 0

19 Number of words for Abstract: 243

20 Number of words for Significance Statement: 111

21 Number of words for Introduction: 747

22 Number of words for Discussion: 2,435

23
24 Acknowledgements:

25 We thank Mohan Gudarvalmiki for help making virus and members of the Cline lab and Ian Wickersham for
26 helpful discussions.

27
28 Conflict of Interest:

29 Authors report no conflict of interest.

30
31 Funding Sources:

32 This work was supported by grants from the US National Institutes of Health (5F32NS071807 to RLF,
33 MH063912 and EY022577 to EMC, EY011261 and EY027437 to HTC), the National Science Foundation DBI-
34 1707261 to EMC, Salk NEI Core (P30 EY019005), and support from the Helen Dorris Foundation to RLF, and
35 an endowment from the Hahn Family Foundation to HTC.

36
37 Keywords:

38 Recombinant rabies virus, retrograde labeling, Xenopus, optic tectum, mesoscale connectomics

49

50 Abstract

51

52 The *Xenopus laevis* experimental system has provided significant insight into the development and plasticity of
53 neural circuits. *Xenopus* neuroscience research would be enhanced by additional tools to study neural circuit
54 structure and function. Rabies viruses are powerful tools to label and manipulate neural circuits and have been
55 widely used to study mesoscale connectomics. Whether rabies virus can be used to transduce neurons and
56 express transgenes in *Xenopus* has not been systematically investigated. Glycoprotein-deleted rabies virus
57 transduces neurons at the axon terminal and retrogradely labels their cell bodies. We show that glycoprotein-
58 deleted rabies virus infects local and projection neurons in the *Xenopus* tadpole when directly injected into
59 brain tissue. Pseudotyping glycoprotein-deleted rabies with EnvA restricts infection to cells with exogenous
60 expression of the EnvA receptor, TVA. EnvA pseudotyped virus specifically infects tadpole neurons with
61 promoter-driven expression of TVA, demonstrating its utility to label targeted neuronal populations. Neuronal
62 cell types are defined by a combination of features including anatomical location, expression of genetic
63 markers, axon projection sites, morphology, and physiological properties. We show that driving TVA
64 expression in one hemisphere and injecting EnvA pseudotyped virus into the contralateral hemisphere,
65 retrogradely labels neurons defined by cell body location and axon projection site. Using this approach, rabies
66 can be used to identify cell types in *Xenopus* brain and simultaneously to express transgenes which enable
67 monitoring or manipulation of neuronal activity. This makes rabies a valuable tool to study the structure and
68 function of neural circuits in *Xenopus*.

69

70

71 Significance Statement

72

73 Studies in *Xenopus* have contributed a great deal to our understanding of brain circuit development and
74 plasticity, regeneration, and hormonal regulation of behavior and metamorphosis. Here, we show that
75 recombinant rabies virus transduces neurons in the *Xenopus* tadpole, enlarging the toolbox that can be applied
76 to studying *Xenopus* brain. Rabies can be used for retrograde labeling and expression of a broad range of
77 transgenes including fluorescent proteins for anatomical tracing and studying neuronal morphology, voltage or
78 calcium indicators to visualize neuronal activity, and photo- or chemosensitive channels to control neuronal
79 activity. The versatility of these tools enables diverse experiments to analyze and manipulate *Xenopus* brain
80 structure and function, including mesoscale connectivity.

81

82

83 Introduction

84

85 Studies in *Xenopus* have yielded insights into research including neural development, plasticity, and
86 regeneration. Progress in these areas of investigation would be facilitated by additional tools to study the
87 structure and function of defined cell types within the *Xenopus* brain. Viruses are an excellent tool for gene
88 manipulation *in vivo* as they can be targeted to specific cell types with high spatio-temporal precision. Viruses
89 can deliver a broad range of transgenes including fluorescent proteins for anatomical tracing and studying
90 neuronal morphology, voltage or calcium indicators to visualize neuronal activity, and photo- or chemosensitive
91 channels to control neuronal activity (Callaway and Luo 2015; Osakada et al., 2011). In *Xenopus*, viral tools
92 are limited. Neither adeno-associated virus (AAV) nor lentivirus transduce brain cells in *Xenopus* (Yamaguchi
93 et al., 2018). Vaccinia virus and vesicular stomatitis virus (VSV) have been used for gene expression in
94 *Xenopus* (Mundell et al., 2015; Wu et al., 1995; Yamaguchi et al., 2018), but expression from Vaccinia is
95 transient and VSV transduction is inefficient (Yamaguchi, personal communication). Therefore, we investigated
96 applications of rabies virus in *Xenopus*.

97
98 Recombinant rabies viruses have been widely used to investigate the structure and function of neural circuits.
99 Depending on the viral variant, rabies virus can be used for retrograde neuroanatomical tracing, transsynaptic
100 tracing, and transgene expression in genetically-defined cell types in specific anatomical locations (Callaway
101 and Luo 2015; Luo et al., 2018; Nassi et al., 2015; Ugolini 2010). Wild-type rabies virions infect neurons at their
102 axon terminals, are transported retrogradely to the soma, and replicate before spreading to presynaptically
103 connected neurons (Schnell et al., 2010). Deletion of the glycoprotein gene from the rabies genome eliminates
104 the ability of viral replication to produce infectious particles. Complementing glycoprotein(G)-deleted rabies
105 virus with a viral envelope protein generates rabies virions which are infectious and transport retrogradely, but
106 do not infect presynaptically connected neurons (Etessami et al., 2000; Mebatsion et al., 1996b; Wickersham
107 et al., 2007a). G-deleted rabies virus infects neurons at their axon terminals and acts as a retrograde vector for
108 expression of transgenes. When the deleted glycoprotein is supplied exogenously in infected neurons (called
109 “*in trans*”), the viral particles spread monosynaptically to presynaptic neurons (Stepien et al., 2010;
110 Wickersham et al., 2007b). Infection of recombinant rabies can be restricted to genetically-defined neuronal
111 populations by pseudotyping with the envelope glycoprotein for the avian sarcoma and leukosis virus, EnvA.
112 Transfecting genetically defined neuronal populations with the receptor for EnvA, TVA, restricts infection to
113 those cell types (Marshall et al., 2010; Wall et al., 2010; Wickersham et al., 2007b; Young et al., 1993),
114 facilitating cell type identification and study. Neuronal subtypes are defined by a combination of features
115 including cell body location, genetic markers, morphology, axonal projections, and physiological properties
116 (Ecker et al., 2017). EnvA pseudotyped rabies can identify neurons simultaneously defined by cell body
117 location through retrograde tracing, genetic control of TVA expression, and axonal projection pattern by
118 localizing viral injection to specific target locations. These rabies viral variants permit flexible investigation into
119 diverse aspects of neural circuit structure and function.

120

121 We examined whether recombinant rabies viruses can be used to express transgenes in *Xenopus laevis* brain.
122 Direct injection of G-deleted rabies virus phenotypically complemented with surface rabies glycoprotein
123 (Conzelmann et al., 1990; Wickersham et al., 2007a) into the tadpole optic tectum infects both local tectal
124 neurons and neurons in contralateral tectum and hindbrain, demonstrating efficient retrograde transport in
125 axons. Previous work has shown that intertectal communication is important for visuomotor behavior in
126 tadpoles (Gambrill et al., 2016). Combining rabies virus injection with post-hoc immunohistochemistry for
127 GABA demonstrated that both excitatory and inhibitory neurons project axons between the two optic tectal
128 lobes, indicating the utility of rabies to study mesoscale connectivity in *Xenopus*. Expression of rabies
129 glycoprotein in *trans* in infected tectal neurons did not result in transsynaptic spread and presynaptic viral
130 infection. Pseudotyping the virus with EnvA restricted infection to neurons transfected with TVA. Using EnvA
131 pseudotyped virus, we achieved retrograde infection of targeted neuronal populations by driving TVA
132 expression with different promoters in afferent neurons and injecting virus into target areas. These results
133 suggest that recombinant rabies viruses could be used to express transgenes in cells triply defined by cell
134 body location, genetics, and axon projection. This combinatorial labeling approach will help uncover cell types
135 in *Xenopus* brain. When paired with the breadth of rabies viral variants that are available to assay neuronal
136 function, this tool will be very useful for investigating the structure and function of neural circuits in this tractable
137 model system.

138

139

140 **Methods**

141

142 **Animals**

143 Albino *Xenopus laevis* tadpoles of either sex were obtained by in-house breeding or purchased from Nasco or
144 Xenopus Express (Cat# ATAD, RRID:XEP_Xla200). Tadpoles were reared in 0.1X Steinberg's solution on a 12
145 hour light / 12 hour dark cycle at 22-23°C unless otherwise stated. Experiments were performed between
146 developmental stages 42-48 (Nieuwkoop and Faber 1956) and tadpoles were anesthetized in 0.02% tricaine
147 methanesulfonate (MS222, Sigma Cat#A5040) before all procedures. All animal protocols were approved by
148 the Institutional Animal Care and Use Committee of The Scripps Research Institute.

149

150 **Preparation and Injection of Pseudotyped Recombinant Rabies Virus**

151 We used envelope glycoprotein (G)-deleted rabies virus expressing EGFP (SADΔG-EGFP) phenotypically
152 complemented with its native glycoprotein, B19G, or pseudotyped with the envelope glycoprotein for the avian
153 sarcoma and leukosis virus, EnvA (Wickersham et al., 2007a; Wickersham et al., 2007b). Viruses were
154 injected at titers between 4.4×10^8 - 1.8×10^9 transducing units (TU)/mL. Viruses were either grown and purified as
155 described in Wickersham et al., (2010) or purchased from the Salk GT3 viral vector core (RRID:SCR_014847).
156 For injection, animals were anesthetized in 0.02% MS222 and virus was pressure injected directly into the

157 optic tectum. Virus was injected into the widest part of the tectal lobe. 0.01% Fast Green dye (Sigma
158 Cat#F7252) was added to viral aliquots prior to injection for visualization and care was taken to ensure that
159 injected virus did not leak into the brain ventricle.

160

161 **Electroporation and Plasmid Constructs**

162 Optic tectal neurons were transfected with TVA800 to mediate SADΔG-EGFP(EnvA) infection, turboRFP
163 (tRFP) to identify TVA-expressing cells, and B19G to generate infectious virions for possible transsynaptic
164 tracing. The CMV promoter was used to drive expression in all neuron types. The vesicular GABA transporter
165 (VGAT) promoter was used to bias expression toward inhibitory neurons (He et al., 2016). In some
166 experiments expression was amplified using the gal/UAS system (Chae et al., 2002). Plasmids were generated
167 to express each protein of interest individually, or to co-express TVA and tRFP. For co-expression, a bi-
168 directional plasmid was used to drive TVA from a sCMV IE94 enhancer/promoter and turboRFP from an
169 independent sCMV promoter. The plasmids used in the study were: CMV::TVA/tRFP
170 (RRID:Addgene_164486), CMV::B19G/tRFP, CMV::B19G (RRID:Addgene_15785), CMV::gal4, VGAT::gal4,
171 UAS::tRFP, UAS::TVA (RRID:Addgene_164487), and UAS::B19G. We transfected neurons using whole-brain
172 or micropipette-mediated electroporation. For whole-brain electroporation, tadpoles were anesthetized in
173 0.02% MS222, plasmids at a concentration of 1ug/ul were pressure injected into the brain ventricle, and then
174 platinum electrodes were placed on each side of the midbrain and voltage pulses were applied across the
175 midbrain (Haas et al., 2002). Whole-brain electroporations transfected cells throughout the rostrocaudal extent
176 of the tectum. For micropipette-mediated electroporation, tadpoles were anesthetized in 0.02% MS222, a glass
177 pipette with filament containing 1ug/ul plasmid DNA was inserted directly into the brain and brief electrical
178 stimulation was delivered by an Axoprotector 800A (Axon Instruments) (Bestman et al., 2006). Micropipette-
179 mediated electroporation transfects one or a few cells near the tip of the micropipette.

180

181 **In Vivo Imaging**

182 Stage 42-48 tadpoles were injected with SADΔG-EGFP(B19G) virus or electroporated with expression
183 constructs and injected with SADΔG-EGFP(EnvA) virus 4 days later. One to seven days following viral
184 injection, animals were anesthetized in 0.02% MS222 and imaged on a PerkinElmer Ultraview Vox spinning
185 disk confocal microscope with a 25X Nikon water-immersion objective lens (1.1 NA). Z-stacks through the
186 entire optic tectum were collected. In some experiments, images were acquired in multiple anatomical
187 locations and montages of Z-projections were created manually.

188

189 **Visual Stimulation**

190 After electroporation and viral injection, tadpoles receiving visual experience were exposed to a simulated
191 motion stimulus consisting of rows of LEDs illuminating in turn (Sin et al., 2002). This visual experience was

192 provided for either (1) 4 hours, 2 days prior to viral injection, or (2) 12 hours overnight, the night before viral
193 injection. The remainder of the time, animals were reared on a normal cycle of 12 hour light / 12 hour dark.

194

195 **Cell Culture**

196 Cell lines were used for western blot and immunohistochemistry to test exogenous expression of B19G. 293T
197 cells (RRID:CVCL_0063) were grown in 90% DMEM (with 4.5g/L D-glucose, L-glutamine, sodium pyruvate,
198 and sodium bicarbonate) and 10% fetal bovine serum at 37°C in 5% CO₂. The XLK-WG cell line is derived
199 from *Xenopus* kidney cells (ATCC Cat#CRL-2527, RRID:CVCL_5655). XLK-WG cells were grown in 60%
200 RPMI 1640 media (with 2mM L-glutamine, 10mM HEPES, 1mM sodium pyruvate, 4.5g/L glucose, and 1.5g/L
201 sodium bicarbonate), 20% fetal bovine serum, and 20% distilled water. XLK-WG cells were maintained at 32°C
202 in 5% CO₂. Cells were transfected with CMV::B19G and α -actin::GFP using calcium phosphate (293T) or
203 Lipofectamine (XLK-WG) and 24-48 hours later cells were collected for western blot or fixed for
204 immunohistochemistry.

205

206 **Western Blots**

207 For western blots of exogenously expressed B19G in cell cultures, cells were scraped from the culture plate of
208 untransfected cells or cells 24 hours after transfection with CMV::B19G and α -actin::GFP and homogenized in
209 RIPA buffer. The membrane fraction was isolated by centrifugation. Small aliquots were taken to measure
210 protein concentration using the BCA Protein Assay kit (Thermo Scientific Cat#23227). Then, 0.1 volume of
211 sample buffer was added to 1 volume of sample and boiled for 5 min. The same amount of protein was loaded
212 from each condition and was separated on an SDS-polyacrylamide gel and proteins were transferred to a
213 nitrocellulose membrane. Membranes were blocked in 5% milk and 0.05% Tween-20 in TBS and then
214 incubated in 1:500 mouse anti-rabies (Millipore Cat#MAB8727, RRID:AB_571110) primary antibody overnight
215 at 4°C. Blots were rinsed and incubated in 1:500 goat anti-mouse HRP-conjugated secondary (BioRad
216 Cat#172-1011, RRID:AB_11125936) at room temperature. β -tubulin (1:750, Sigma Cat#T8535,
217 RRID:AB_261795) was used as a loading control. An ECL chemiluminescence kit (Thermo Scientific
218 Cat#32106) was used to visualize labeling.

219

220 **Immunohistochemistry**

221 To investigate whether membrane expression of B19G was observed in XLK-WG cells in vitro, we performed
222 immunohistochemistry without permeabilization. Two days after transfection with CMV::B19G and α -
223 actin::GFP, cells were fixed in 4% paraformaldehyde for 15 min and blocked in 10% BSA for 45 minutes at
224 room temperature. Next, coverslips were incubated in 1:2000 mouse anti-rabies (Millipore Cat# MAD8727,
225 RRID:AB_571110) in 3% BSA overnight at 4°C, followed by 45 min in 1:200 donkey anti-mouse Alexa 647
226 (ThermoFisher Cat#A-31571, RRID:AB_162542). As a control for primary antibody specificity,
227 immunohistochemistry was also performed on XLK-WG transfected only with α -actin::GFP. Coverslips were

228 mounted in Prolong Diamond Antifade Mountant (ThermoFisher Cat#P36970) and imaged with a Nikon A1R
229 confocal microscope with a 25X Nikon water-immersion objective lens (1.1 NA).

230

231 To investigate exogenous expression of B19 glycoprotein in vivo, tadpoles were electroporated with
232 CMV::B19G/tRFP and fixed 3-4 days later for immunohistochemistry. Tadpoles were anesthetized with 0.02%
233 MS222, immersed in 4% paraformaldehyde, and fixed using two bouts of microwave fixation at 150 W for 1
234 min followed by overnight fixation at 4°C. Brains were dissected, embedded in a gelatin-albumin mixture, and
235 sectioned at 40-50um on a vibratome. Sections were blocked and permeabilized in 5% normal donkey serum
236 and 1% Triton X-100 for 1h at room temperature. Then, sections were incubated in 1:500 mouse anti-rabies
237 (Millipore Cat#MAB8727, RRID:AB_571110) for 2 days at 4°C followed by 2h in 1:200 goat anti-mouse Alexa
238 405 (ThermoFisher Cat#A-31553, RRID:AB_221604) or Alexa 488 (ThermoFisher Cat#A-11001,
239 RRID:AB_2534069) at room temperature. Sections were mounted in Gel mount (Accurate) and imaged with a
240 PerkinElmer Ultraview Vox spinning disk confocal microscope with a 25X Nikon water-immersion objective lens
241 (1.1 NA).

242

243 **Results**

244

245 **Recombinant rabies virus infects *Xenopus* neurons**

246 To test whether rabies virus infects neurons in the *Xenopus* tadpole, we used the recombinant rabies virus
247 SADΔG-EGFP in which the glycoprotein from the SAD B19 rabies strain is deleted and replaced with EGFP
248 (Conzelmann et al., 1990; Wickersham et al., 2007a). Amplifying SADΔG-EGFP using complementing cell
249 lines which express an envelope glycoprotein makes infectious viral particles, but the virus generates virions
250 which lack glycoprotein and cannot spread. We used SADΔG-EGFP phenotypically complemented with its
251 native glycoprotein, B19G, or pseudotyped with the envelope glycoprotein for the avian sarcoma and leukemia
252 virus, EnvA (Wickersham et al., 2007a; Wickersham et al., 2007b). Infection with SADΔG-EGFP(B19G) virus
253 occurs in cells expressing any endogenous B19G receptor. SADΔG-EGFP(EnvA) virus requires expression of
254 the TVA receptor to mediate infection. TVA is found only in birds and requires exogenous expression,
255 permitting experimental control of the cell types infected (Federspiel et al., 1994; Wickersham et al., 2007b;
256 Young et al., 1993). We tested whether SADΔG-EGFP(B19G) and SADΔG-EGFP(EnvA) viruses infect
257 neurons in the *Xenopus* tadpole optic tectum (Figure 1A). Our first goal was to evaluate a variety of conditions
258 to ascertain when viral infection occurred. As an initial metric to screen the degree of infection, we quantified
259 the proportion of animals with EGFP-expressing rabies infected neurons.

260

261 SADΔG-EGFP(B19G) virus infects neurons at axon terminals and retrogradely labels infected somata with
262 EGFP (Wickersham et al., 2007a). In stage 46-48 tadpoles, we found that injection of SADΔG-EGFP(B19G)
263 virus directly into one optic tectal lobe resulted in robust EGFP expression near the injection site (Figure 1B,

264 n=28/33 tadpoles, 85% infected), presumably from uptake at local axon terminals. We found that injection of
265 SADΔG-EGFP(B19G) into the ventricle produced widespread infection. Therefore, care was taken to ensure
266 that virus was injected directly into brain tissue without leaking into the ventricle in all experiments. Tadpoles
267 are reared at 22°C and we postulated that this decreased body temperature might lead to decreased efficiency
268 of viral infection compared to warm-blooded vertebrates, like rodents, in which rabies virus has been used
269 extensively. Short term incubations at increased temperature have previously been shown to improve infection
270 efficiency in *Xenopus* with other viruses (Dutton et al., 2009) and with G-deleted rabies in fish (Dohaku et al.,
271 2019). To test whether increasing the rearing temperature increased the proportion of tadpoles infected with
272 rabies virus, we injected animals with SADΔG-EGFP(B19G) virus and incubated them at 26°C or 28°C for 4
273 hours immediately following viral injection and again 24 hours later. Tadpoles were housed at 22°C for the
274 remainder of the experiment. Five to seven days later, we found that 83% of tadpoles (n=10/12 tadpoles)
275 reared continuously at 22°C were infected, while 64% of tadpoles (n=7/11 tadpoles) temporarily incubated at
276 26-28°C were infected, suggesting that increased temperature did not impact infection rates ($p=0.37_a$). In the
277 infected animals, the number and brightness of EGFP⁺ neurons did not appear different between the groups.
278 These results demonstrate that at normal rearing temperature, a large majority of tadpoles have infected
279 neurons with robust expression of EGFP following injection of B19G phenotypically complemented rabies
280 virus.

281

282 Next, we tested whether TVA expression could be used to mediate infection of SADΔG-EGFP(EnvA) virus in
283 targeted neuronal populations. We transfected tectal neurons with a dual CMV promoter expression plasmid to
284 drive pan-neuronal TVA and turboRFP expression (CMV::TVA/tRFP) using whole-brain electroporation (Haas
285 et al., 2002). Four days later, when tRFP expression was strong, we injected SADΔG-EGFP(EnvA) virus
286 directly into the transfected optic tectum. Three days after viral injection we observed a subset of tRFP⁺
287 neurons were infected with pseudotyped rabies virus, as identified by EGFP expression (Figure 1C; n=41/65
288 tadpoles, 63% infected). Therefore, we achieved infection and robust EGFP expression in a majority of animals
289 with SADΔG-EGFP(EnvA) virus.

290

291 To test whether pseudotyped rabies virus-mediated infection might vary with the developmental stage of the
292 tadpoles, we used whole-brain electroporation to transfect tadpoles ranging from stages 42-48 with
293 CMV::TVA/tRFP and injected virus into the tectum 4 days later. Infection was most efficient when tadpoles
294 were electroporated between stages 44-48 (Figure 1D), which are ideal stages for performing studies of
295 development and experience-dependent plasticity in tadpoles *in vivo*.

296

297 In mouse, infection with SADΔG-EGFP(EnvA) virus requires exogenous TVA expression and there is no
298 infection in the absence of TVA (Wall et al., 2010; Wickersham et al., 2007b). However, we observed a number
299 of EGFP⁺ cells without detectable expression of TVA/tRFP in these experiments (Figure 1C). To determine

300 whether TVA expression is required for infection with SADΔG-EGFP(EnvA) virus in *Xenopus*, we injected
301 SADΔG-EGFP(EnvA) virus into the tectum of untransfected tadpoles. TVA-expressing animals were also
302 injected with the same viral aliquot as a positive control and animals were imaged using identical imaging
303 parameters 6 days later. While the majority of TVA-expressing tadpoles were infected 6 days after viral
304 injection ($n=13/18$ tadpoles), we did not observe any EGFP⁺ cells in the absence of TVA (Figure 1E; $n=0/21$
305 tadpoles). This result indicates that the virus cannot infect *Xenopus* neurons in the absence of the TVA
306 receptor and suggests that EGFP⁺ cells that we observed in TVA/tRFP transfected animals express a low level
307 of TVA which is sufficient to mediate infection, but the tRFP is below detection threshold. These so-called
308 “invisible TVA” neurons have been noted in other studies, in particular when using Cre-dependent gene
309 expression which can have some leakage, because of the very sensitive interaction between EnvA and TVA
310 (Callaway and Luo 2015; Hafner et al., 2019; Lavin et al., 2020). Increasing expression of co-transfected
311 fluorescent proteins in TVA-expressing neurons and reducing the affinity of EnvA for TVA by mutating TVA
312 have been used to reduce the number of invisible TVA cells (Miyamichi et al., 2013).

313
314 To assess whether increasing tRFP expression would decrease the number of invisible TVA cells, we used the
315 gal4-UAS bipartite transcriptional system to amplify gene expression (Chae et al., 2002; Hirsch et al., 2002). In
316 addition to using the CMV promoter, we drove TVA and tRFP expression using the VGAT promoter, which has
317 previously been shown to increase transfection of inhibitory neurons in the tectum (He et al., 2016). The
318 proportion of excitatory:inhibitory neurons in the optic tectum is 70:30 (Miraucourt et al., 2012). Using post-hoc
319 immunohistochemistry for GABA, it has been demonstrated that the VGAT promoter increases expression in
320 inhibitory neurons so that the transfected population is 50:50 excitatory:inhibitory (He et al., 2016). Co-
321 electroporation of VGAT::gal4 or CMV::gal4 with UAS::TVA, and UAS::tRFP into the tectum, followed by
322 injection of SADΔG-EGFP(EnvA) virus 4 days later resulted in infection in the majority of tadpoles (Figure 1F;
323 $n=25$ tadpoles, 60% infected). The proportion of tadpoles with infected neurons was similar between the two
324 promoters (CMV::gal4: $n=3/4$ tadpoles; VGAT::gal4: $n=12/21$ tadpoles; $p=0.63_b$). We observed a significant
325 decrease in the number of invisible TVA neurons which were infected by SADΔG-EGFP(EnvA) virus when
326 TVA and tRFP expression was amplified using the gal4-UAS system (Figure 1G). When animals were
327 electroporated with CMV::TVA/tRFP and injected with SADΔG-EGFP(EnvA) virus 4 days later, an average of
328 85% of EGFP⁺ neurons per animal lacked detectable tRFP expression. In contrast, electroporating tadpoles
329 with CMV::gal4 or VGAT::gal4 along with UAS::TVA and UAS::tRFP, resulted in only 28% of EGFP⁺ neurons
330 which lacked detectable tRFP ($p<0.0001_c$). In addition, these data demonstrate that different promoters can be
331 used to target infection with SADΔG-EGFP(EnvA) showing its utility to target genetically defined neuronal
332 populations.

333
334 To test whether targeting electroporation to a few cells per tectum could reduce the number of invisible TVA
335 neurons, we electroporated tectal cells sparsely using a micropipette (Bestman et al., 2006). For this

336 experiment we used CMV::TVA/tRFP because micropipette-mediated electroporation of multiple plasmids is
337 inefficient. We electroporated 3-4 sites within one tectum. Four days later, we injected animals with successful
338 targeted TVA/turboRFP electroporation with SADΔG-EGFP(EnvA) virus and imaged the animals five days
339 later. While the majority of animals were infected (77%, n=13/17 tadpoles), they still had a number of EGFP-
340 only cells present (Figure 1H). Next, we limited electroporation even further by electroporating only one site per
341 tectum with CMV::TVA/tRFP and screened for animals with a single tRFP⁺ cell. These tadpoles were injected
342 with SADΔG-EGFP(EnvA) virus four days after electroporation. However, 4-7 days after viral injection, no
343 infected cells were detected (n=11 tadpoles). These data demonstrate that using targeted micropipette
344 electroporation did not limit viral infection to cells with detectable tRFP expression, however these data do
345 show that increasing tRFP co-expression in TVA⁺ neurons decreased the proportion of infected EGFP-only
346 cells but did not eliminate them.

347

348 Together, these results demonstrate that recombinant rabies virus infects neurons in *Xenopus* tadpoles. Viral
349 injection of B19G phenotypically complemented virus produces widespread infection and strong transgene
350 expression in the vast majority of animals. Furthermore, pairing promoter-driven expression of TVA with
351 injection of EnvA pseudotyped rabies virus can be used to express genes of interest in targeted neuronal
352 populations in *Xenopus* tadpoles.

353

354 **Lack of presynaptic transfer of pseudotyped rabies virus**

355 Pseudotyped recombinant rabies virus will undergo retrograde monosynaptic transfer when infected neurons
356 are supplied with rabies glycoprotein, B19G *in trans* (Wickersham et al., 2007b). Viral particles which bud from
357 infected neurons transcomplemented with B19G have glycoprotein on their surface and infect presynaptically
358 connected cells (Figure 2A). Following viral injection, neurons transfected with TVA/tRFP and directly infected
359 by virus injection would be expected to express both tRFP and EGFP, while neurons infected via presynaptic
360 transfer would express EGFP alone (Figure 2A).

361

362 Since we observed EGFP-only cells in the absence of B19G expression (Figures 1C-D), the presence of local
363 EGFP-only cells could not be used as an indication of presynaptic infection under these conditions. We
364 reasoned that if presynaptic transfer occurred in the presence of B19G expression, we would detect an
365 increase in the number of EGFP⁺ neurons over time as virions spread presynaptically and presynaptic neurons
366 began to express EGFP. We electroporated tadpoles with either TVA/tRFP alone, or both TVA/tRFP and B19G
367 and injected SADΔG-EGFP(EnvA) virus 4 days later. We performed *in vivo* time lapse imaging at 3 and 6 days
368 following virus injection and quantified the number of EGFP⁺ cells at both time points (Figure 2B). On average,
369 there was a 1.46-fold increase in the number of EGFP⁺ cells from 3 to 6 days in TVA/tRFP/B19G-expressing
370 animals. Similarly, in animals which expressed only TVA/tRFP, and were thus incapable of presynaptic spread,
371 there was a 1.88-fold increase in the number of EGFP⁺ neurons from 3 to 6 days after infection ($p=0.74_d$)

372 (Figure 2C). This result demonstrated that an increase in EGFP-expressing cells over time was not necessarily
373 indicative of presynaptic transfer of virus.

374

375 Next, we looked for evidence of presynaptic infection by investigating whether EGFP⁺ neurons were visible
376 outside of the injected tectal lobe. Following unilateral electroporation of TVA and B19G into a single tectal
377 lobe, injection of SADΔG-EGFP(EnvA) virus into the transfected tectal lobe would be expected to produce
378 presynaptic infection in several known presynaptic brain areas including the contralateral tectum and hindbrain
379 (Gambrill et al., 2016; Hiramoto and Cline 2009). However, when SADΔG-EGFP(EnvA) was injected into the
380 transfected tectal lobe, no EGFP⁺ neurons were ever observed in known presynaptic brain regions (data not
381 shown). While trans-synaptic infection occurs in mammalian systems within a week (Wall et al., 2010), this
382 process may be slower in non-mammalian vertebrates reared at lower temperatures. Since survival and health
383 of rabies infected neurons begins to diminish after about 2 weeks (Wickersham et al., 2007a), we looked for
384 presynaptically infected neurons up to 10 days following viral injection in a subset of tadpoles, but still failed to
385 observe EGFP⁺ neurons in presynaptic brain regions (n=6 tadpoles, data not shown). Taken together, the
386 results of these two experiments suggest that trans-synaptic infection of cells in the tadpole does not occur
387 under the conditions we tested.

388

389 **Lack of presynaptic infection may be due to insufficient glycoprotein expression**

390 The most likely explanations for a lack of presynaptic infection are (1) presynaptic terminals do not contain the
391 receptor(s) necessary for viral uptake, (2) the virus is not packaged and transported appropriately, (3)
392 synapses are too weak to mediate presynaptic infection, (4) electroporated B19G is not expressed sufficiently
393 or in the correct place to coat budding virions, or (5) the virus is not released at the appropriate location. We
394 ruled out the first possibility because B19G phenotypically complemented virus infects tectal neurons,
395 demonstrating that the B19G receptor(s) exist in *Xenopus* tadpoles at this stage. We tested two of the other
396 possibilities to understand why we did not detect transsynaptic infection and to identify strategies for
397 improvement in the future.

398

399 There has been speculation that the extent of presynaptic spread might depend on the strength or number of
400 synapses (Callaway 2008). It is possible that the synaptic connections in young tadpoles might be too weak to
401 efficiently mediate presynaptic infection. To test this, we exposed tadpoles to a visual stimulus prior to viral
402 injection, which has previously been shown to increase synaptic strength (Aizenman and Cline 2007; Ruthazer
403 et al., 2006). We electroporated tadpoles with VGAT::gal4, UAS::TVA, UAS::tRFP, and UAS::B19G in one
404 tectal lobe and then exposed them to visual experience (VE) for either: (1) Four hours of VE 2 days prior to
405 viral injection, or (2) 12 hours of VE the night before viral injection. Similar to other experiments, 64% of
406 tadpoles (n=9/14 tadpoles) provided with visual stimulus were infected by SADΔG-EGFP(EnvA) virus.
407 However, we did not observe EGFP⁺ cells outside of the injected tectal lobe in any of the groups (data not

408 shown) suggesting that increasing synaptic strength with these protocols is insufficient to produce presynaptic
409 transfer of virus.

410

411 For presynaptic infection to occur, B19G expression is required on the cell membrane so that it coats the
412 surface of budded viral particles. In addition, surface B19G expression increases the number of virions which
413 bud from infected neurons (Mebatsion et al., 1996a). To test the possibility that B19G is not expressed
414 sufficiently in transcomplemented cells, we first assessed expression of B19G in vitro. We transfected 293T
415 cells with CMV::B19G and α -actin::GFP. One day after transfection, we harvested cells and did western blots
416 on membrane fractions using anti-rabies glycoprotein antibody previously shown to detect B19G (Beier et al.,
417 2019). We detected B19G in the membrane fraction of 293T cells, but no signal was found in untransfected
418 cells (Figure 3A). To test whether B19G expression occurs in frog cells, we transfected XLK-WG Xenopus
419 kidney cells with CMV::B19G and α -actin::GFP, harvested cells one day after transfection, and did western
420 blots on membrane fractions. While there was a band of similar size to rabies glycoprotein found in both
421 transfected and untransfected cells, we observed an additional band specifically in the transfected XLK-WG
422 cells (Figure 3B). Next, we performed immunohistochemistry for the rabies glycoprotein in CMV::B19G-
423 expressing XLK-WG cells. Cells were transfected with CMV::B19G and α -actin::GFP and fixed for
424 immunohistochemistry 48 hours later. We found that B19G was expressed on the membrane of XLK-WG cells
425 using non-permeabilized immunohistochemistry conditions with anti-rabies glycoprotein antibody (Figure 3C).
426 In contrast, XLK-WG cells transfected with α -actin::GFP alone and imaged using identical parameters had no
427 detectable staining with the anti-rabies glycoprotein antibody. Together, these results indicate that B19G can
428 be expressed on the cell membrane in Xenopus cells in vitro.

429

430 Finally, we assessed the expression of B19G in tadpoles in vivo. We electroporated CMV::B19G/tRFP and
431 examined expression of the glycoprotein using immunohistochemistry. Four days following electroporation, we
432 fixed the animals, dissected and embedded their brains, sectioned them on a vibratome, and performed
433 immunohistochemistry with anti-rabies glycoprotein antibody. Expression of B19G was either observed at low
434 levels (Figure 3D) or not at all (data not shown). When B19G signal was present, it was observed in the
435 membrane of the apical cell body and in the proximal dendrite. By comparison, B19G expression in XLK-WG
436 cells appeared much stronger and more uniform around the cell membrane. While we cannot rule out
437 differences in antibody penetration in intact tissue compared to culture, these results are consistent with
438 insufficient expression of B19G in vivo contributing to the lack of presynaptic spread of rabies virus.

439

440 **Retrograde labeling of neural circuits with recombinant rabies virus**

441 In mammals, recombinant rabies virus can be used as a retrograde tracer since it infects at the axon terminal
442 and is retrogradely transported to the cell soma. We tested the utility of using recombinant rabies virus as a
443 retrograde tracer in Xenopus tadpoles. As demonstrated in Figure 1B, unilateral injections of SADΔG-

444 EGFP(B19G) virus into the optic tectum transduced local axon terminals and yielded robust labeling at the
445 injection site. In 43% of the infected animals (n=15/35 tadpoles), we also observed retrogradely infected
446 EGFP⁺ cells in other brain regions which project to the optic tectum (Figure 4A). From these data we generated
447 a schematic of neurons which were retrogradely labeled by unilateral tectal injection of SADΔG-EGFP(B19G)
448 virus (Figure 4B). We found retrograde labeling of neurons in regions known to project to the optic tectum
449 including the contralateral optic tectal lobe, hindbrain, pre-tectum and forebrain, as well as the ipsilateral
450 hindbrain. EGFP⁺ cells were also present in very high numbers in the ipsilateral pre-tectum making them
451 difficult to count and were not included in the schematic. Retinal ganglion cells are known to be a primary
452 source of input to the optic tectum, but no EGFP was observed in the optic chiasm and the eye was not
453 examined in these experiments. It is possible that viral injections were made too deep to label the superficially
454 located retinal ganglion cell axons, or that rabies poorly infects the axon terminals of some cell types in the
455 tadpole. Nonetheless, we found robust infection in several known presynaptic areas demonstrating that rabies
456 can transport between brain regions and act as a retrograde tracer in tadpoles.

457
458 Combining retrograde tracing with immunohistochemistry can provide information about the cell types which
459 project to a target region of interest. For example, neurons which project between the tectal hemispheres are
460 consistently labeled by injection of SADΔG-EGFP(B19G) virus. The development and function of intertectal
461 inputs in tadpoles has only recently begun to be studied (Gambrill et al., 2016; Gambrill et al., 2018). Whether
462 intertectal inputs are excitatory and/or inhibitory will have a large impact on how they contribute to the function
463 of the tectal circuit. To ascertain whether intertectal neurons are excitatory or inhibitory, we performed live
464 imaging of tadpoles seven days after injection of SADΔG-EGFP(B19G) virus into the right tectal lobe to screen
465 for infection, and then fixed infected tadpoles and performed immunohistochemistry on brain sections with an
466 anti-GABA antibody (Figure 4C). At this developmental stage, GABA immunohistochemistry can be used to
467 determine whether neurons are excitatory or inhibitory because GABA immuno-negative neurons are positive
468 for the excitatory neuronal marker CaMKII (Miraucourt et al., 2012). Using this strategy, the ratio of excitatory
469 to inhibitory intertectal neurons was found to be 3:1 (Gambrill et al., 2016), closely matching the overall
470 proportion of these neuronal types in the optic tectum at this stage (Miraucourt et al., 2012). This experiment
471 demonstrates the utility of retrograde rabies infection of afferent neurons in the tadpole to explore questions of
472 circuit composition.

473
474 A complementary strategy to the one described above is to use cell-type specific expression of EnvA to control
475 the cell types which become retrogradely infected with pseudotyped rabies (Dohaku et al., 2019). We
476 assessed whether retrograde tracing with pseudotyped rabies virus can be combined with promoter-driven
477 expression of TVA in distant afferent neurons in the tadpole. We electroporated the left tectal lobe with
478 TVA/tRFP driven by the CMV or VGAT promoter and then injected SADΔG-EGFP(EnvA) virus in the left or
479 right tectal lobe four days later. As observed previously (Figure 1), 59% of tadpoles (n=16/27 tadpoles) injected

480 with virus in the transfected tectal lobe had EGFP⁺ cells as a result of local viral transduction. We also found
481 that 16% of tadpoles (n=5/32 tadpoles) injected with SADΔG-EGFP(EnvA) virus in the tectal lobe contralateral
482 to TVA/tRFP transfection had EGFP⁺ cells in the transfected tectal lobe (Figures 4D-E). This result suggests
483 that electroporated TVA is expressed on the afferent axons of transfected neurons and SADΔG-EGFP(EnvA)
484 virus can infect neurons via those axons when injected into target areas. In contrast, SADΔG-EGFP(EnvA)
485 virus injection into the transfected right tectal lobe never resulted in EGFP⁺ cells in the untransfected left tectal
486 lobe (n=0/27 tadpoles). This demonstrates that retrograde infection with SADΔG-EGFP(EnvA) required axonal
487 expression of TVA.

488

489 Together, these experiments demonstrate that recombinant rabies virus can be used to express genes of
490 interest in the *Xenopus* tadpole. SADΔG-EGFP(B19G) retrogradely infects both excitatory and inhibitory
491 neurons in several brain regions. SADΔG-EGFP(EnvA) can be paired with promoter-driven expression of TVA
492 to label targeted populations of neurons defined by cell body location and axon projection. These viral variants
493 provide the flexibility to identify and manipulate gene expression in projection neurons in both a pan-neuronal
494 and cell-type specific manner.

495

496

497 **Discussion**

498

499 Here we demonstrate that recombinant rabies virus infects neurons in the *Xenopus* tadpole brain. B19G
500 phenotypically complemented virus infects neurons via its endogenous receptor, while EnvA pseudotyped virus
501 infects subpopulations of neurons by targeted expression of the TVA receptor. Both viruses resulted in
502 infection in the majority of injected tadpoles between developmental stages 44-48. They produced robust
503 transgene expression in the cell body and, sometimes, EGFP expression was bright throughout the cellular
504 processes as well. While we do not have evidence of transneuronal spread of rabies in the tadpole, the use of
505 rabies in *Xenopus* to combine retrograde labeling from specific axon projection sites with transgene expression
506 will facilitate exciting new research into mesoscale connectomics and the function of neural circuits in a
507 tractable model system (Zeng 2018).

508

509 **Virus-mediated gene expression in non-mammalian vertebrates**

510 Virus-mediated gene expression in non-mammalian vertebrates has had mixed results. AAV and lentivirus,
511 which have been used with great success in mammals (Haery et al., 2019; Nassi et al., 2015; Parr-Brownlie et
512 al., 2015), infect *Xenopus* and zebrafish either inconsistently or not at all (Yamaguchi et al., 2018; Zhu et al.,
513 2009). *Xenopus* express two homologues of the Cosackie and Adenovirus Receptor (CAR) rendering them
514 susceptible to infection by adenovirus and adenovirus-mediated expression of EGFP lasts for at least 10 days
515 in non-neuronal tissue (Dutton et al., 2009; Kawakami et al., 2006). However, tadpoles must be maintained at

516 increased temperature immediately following viral injection for infection to occur and it is not currently known
517 whether neurons in the central nervous system can be infected by adenovirus. Vaccinia is a DNA virus with
518 large packaging capacity that widely infects tadpole neurons when injected into the brain ventricle and can be
519 targeted to specific brain regions when directly injected into brain tissue (Wu et al., 1995). Vaccinia produces
520 robust transgene expression at normal rearing temperature, however transgene expression is transient,
521 decreasing over 10 days after infection. The versatility of vaccinia is limited because it cannot be restricted to
522 specific cell types using promoters. Vesicular stomatitis virus (VSV), like rabies, is an enveloped negative-
523 sense RNA virus (Nassi et al., 2015) that can reportedly infect neurons in both *Xenopus* and zebrafish
524 (Mundell et al., 2015; Yamaguchi et al., 2018). In zebrafish, VSV encoding the VSV glycoprotein VSV(VSV-G)
525 infects neurons and undergoes anterograde transneuronal spread, while VSV encoding the rabies glycoprotein
526 VSV(RABV-G) infects neurons and undergoes retrograde transneuronal spread (Ma et al., 2019; Mundell et
527 al., 2015). Yamaguchi et al., (2018) found that direct injection of VSV(VSV-G) and VSV(RABV-G) into the
528 brains of *Xenopus* frogs and tadpoles infects neurons but does not spread transneuronally. In contrast,
529 Mundell et al., (2015) reported anterograde transneuronal transfer of VSV(VSV-G) from the eye to the brain in
530 *Xenopus* tadpoles, but the data were not shown. It is not clear what accounts for the difference between these
531 findings, but both the age of the animals and the site of viral injection differed and could contribute to the
532 variability in the results. These studies demonstrate that while viral tools for *Xenopus* are available, rabies is an
533 attractive addition to the viral toolbox.

534

535 **Lack of presynaptic viral spread in *Xenopus***

536 We were unable to detect retrograde transneuronal spread of pseudotyped rabies in *Xenopus* tadpoles.
537 Similarly, transneuronal transfer was not observed in adult *Xenopus* frogs injected with recombinant VSV
538 encoding the rabies glycoprotein (Yamaguchi et al., 2018). Transneuronal transfer of rabies requires replication
539 and transport of rabies virions, budding of rabies virions from the postsynaptic cell, expression of glycoprotein
540 on the surface of budded virions, and presynaptic expression of the rabies glycoprotein receptor. We observed
541 infection with SADΔG-EGFP(B19G) demonstrating that the rabies glycoprotein receptor is expressed in
542 *Xenopus* tadpole brain. Given the wide range of neurons which can be infected by rabies in mammals, the
543 glycoprotein receptor is thought to be ubiquitous (Kelly and Strick 2000). NCAM, P75^{ntr}, and mGluR2 have
544 been identified as potential receptors for rabies glycoprotein in the brain (Thoulouze et al., 1998; Tuffereau et
545 al., 1998; Wang et al., 2018), although P75^{ntr} is not required for infection (Tuffereau et al., 2007). All three are
546 also expressed in the *Xenopus* brain to mediate infection with SADΔG-EGFP(B19G) in tadpoles (Session et
547 al., 2016). Following infection at the axon terminal, rabies virions are transported to the cell body for replication,
548 and then spread to dendrites for release. Inefficient viral replication or transport of rabies virions out to the
549 dendrites could contribute to a lack of presynaptic infection. Based on the level of EGFP expression from the
550 virus, replication of rabies virus may be diminished in our system compared to mammals. In mammalian
551 systems, neurons infected with recombinant rabies invariably express very high levels of fluorescent protein

552 making the entire neuron visible (Marshall et al., 2010; Wickersham et al., 2007a). We sometimes observed
553 beautiful EGFP labeling throughout entire neuronal arbors, but often, only cell bodies were labeled by EGFP.
554 This could be a result of inefficient viral replication at the colder temperatures (~20°C) required for rearing
555 *Xenopus*. Future work using recombinant rabies in *Xenopus* should take this variable into account.
556 Manipulations that require labeling the entire neuronal arbor or high expression levels of genes of interest may
557 be accomplished by incorporating amplification mechanisms, such as gal4-UAS or Cre-recombinase.
558 Increasing the rearing temperature in *Xenopus* has been shown to facilitate infection with adenovirus (Dutton
559 et al., 2009) and rearing zebrafish between 34-35.5°C was required for transneuronal transfer of SADΔG-
560 EGFP(EnvA) (Dohaku et al., 2019). We found that a modest, short term increase in rearing temperature did not
561 increase the percentage of animals infected by rabies virus, however further experiments exploring varying the
562 rearing temperature of tadpoles might improve transgene expression or transneuronal transfer.

563
564 Two likely explanations for a lack of transneuronal infection in *Xenopus* tadpole brain are insufficient
565 expression of rabies glycoprotein and/or problems with viral budding. We did not assess whether the virus
566 buds appropriately from *Xenopus* neurons. Two possible ways to investigate this in the future are to infect
567 *Xenopus* cells in vitro and then measure viral proteins in collected culture media or to perform electron
568 microscopy of infected tectal neurons in vivo. We assessed the expression of rabies glycoprotein in *Xenopus*
569 neurons both in vitro and in vivo. Exogenously expressed glycoprotein was detected on the membrane of XLK-
570 WG cells in vitro by western blot and immunocytochemistry. However, there was very little expression detected
571 by immunohistochemistry in tectal neurons following electroporation in vivo. Yamaguchi et al., (2018)
572 demonstrated that B19G incorporated into the VSV genome was also insufficient to produce transneuronal
573 transfer, suggesting that the difficulty of expressing B19G in vivo in *Xenopus* is not specific to electroporation.
574 While viral particles lacking the glycoprotein are capable of budding from cells, presence of the glycoprotein
575 increases budding of viral particles by 30-fold (Mebatsion et al., 1996a). Therefore, improving glycoprotein
576 expression would not only facilitate binding of viral particles to the presynaptic terminal during transneuronal
577 spread, but it would also improve budding of viral particles from infected postsynaptic neurons. There are
578 several possibilities which could explain poor glycoprotein expression and ways that it could be improved.
579 Rabies glycoprotein has multiple glycosylation sites and at least one of them needs to be glycosylated for
580 expression of glycoprotein on the membrane (Conzelmann et al., 1990; Dietzschold 1977; Shakin-Eshleman et
581 al., 1992). Previously, injection of rabies glycoprotein RNA into *Xenopus* oocytes was found to produce an
582 unglycosylated protein product (Wunner et al., 1980). Whether rabies glycoprotein is glycosylated in *Xenopus*
583 in vivo remains to be investigated. Expressing the glycoprotein from a different strain of rabies could be a way
584 to achieve transneuronal tracing in *Xenopus*. The pathogenicity of different rabies strains is determined, in
585 large part, by their glycoproteins. The glycoproteins are expressed at different levels on the cell surface and
586 contribute to different rates of viral replication and spread (Dietzschold et al., 2008). Furthermore, the
587 distribution of presynaptic neurons labeled following viral injection depends on which rabies strain the

588 glycoprotein is taken from, suggesting that the tropism may vary between different glycoproteins (Yan et al.,
589 2002). The Challenge Virus Standard (CVS) strain of rabies has also been used extensively for transneuronal
590 tracing (Astic et al., 1993; Kelly and Strick 2000; Reardon et al., 2016; Ugolini 1995). In mice, G-deleted CVS-
591 N2c virus phenotypically complemented with N2c-G or G-deleted SAD B19 virus pseudotyped with N2c-G
592 infect about 10-fold more presynaptic neurons compared to SAD Δ G-EGFP(B19G) (Reardon et al., 2016; Zhu
593 et al., 2020). A chimeric glycoprotein containing the cytoplasmic domain of the parent SAD B19 glycoprotein
594 and the extracellular domain of the glycoprotein from the Pasteur Virus (PV) strain of rabies also resulted in
595 higher presynaptic infection in mouse brain (Kim et al., 2016). The efficacy of presynaptic infection increased
596 even further when the chimeric glycoprotein was codon optimized, yielding 20-fold more presynaptic neurons
597 compared to non-optimized B19G (Kim et al., 2016). Optimizing codon usage for the desired species has been
598 shown to increase glycoprotein expression by 2-fold (CVS-N2c G) (Wirblich and Schnell 2011). Using
599 glycoproteins from different strains which are codon optimized for *Xenopus* has the potential to improve
600 glycoprotein expression and transneuronal spread.

601

602 **Mesoscale brain circuitry analysis with rabies virus**

603 Neuroanatomical brain connectivity studies have helped to uncover the structure of individual neurons and
604 neuronal circuits, while expression of transgenes in neurons allows for their visualization and manipulation
605 (Luo et al., 2018; Nassi et al., 2015; Vercelli et al., 2000; Zeng 2018). These techniques have contributed
606 greatly to our understanding of the brain. Rabies combines these tools into a single reagent capable of
607 retrogradely labeling neurons based on axonal projections and simultaneously expressing transgenes to
608 visualize or manipulate neuronal activity (Nassi et al., 2015; Osakada et al., 2011). The widespread adoption of
609 rabies for mesoscale circuit analysis has led to the creation of a plethora of viral variants which could be used
610 in *Xenopus*.

611

612 Cells infected with recombinant rabies virus engineered to express fluorescent proteins and phenotypically
613 complemented with B19G are intensely labeled as a result of viral replication. Combining rabies retrograde
614 tracing with posthoc immunohistochemistry reveals the cell types which contribute to neural circuits and
615 suggests that application of rabies virus to study mesoscale connectomics in *Xenopus* will generate new
616 insights into circuit components and circuit function. For instance, we recently investigated the development
617 and function of a direct intertectal projection in tadpoles. Using rabies virus injection followed by posthoc
618 immunohistochemistry, we found that both excitatory and inhibitory tectal neurons contribute to intertectal
619 communication, which has major implications for how this neural circuit contributes to tectal function (Gambrill
620 et al., 2016). We found that injection of SAD Δ G-EGFP(B19G) directly into the brain ventricle resulted in
621 widespread infection near the injection site. This strategy could be exploited to infect neurons and express
622 genes of interest when retrograde tracing from a specific target is not needed. Rabies virus variants are
623 available which drive expression of many fluorescent proteins including GFP, DsRed, mCherry, and BFP

624 (Osakada et al., 2011). In principle, intersectional analysis using simultaneous injection of rabies variants
625 expressing different color fluorescent proteins into different target areas could be used to assess the
626 distribution of neurons projecting to those different targets. In addition, by identifying doubly- or triply-labeled
627 neurons, the degree to which single neurons send axon collaterals to multiple targets can be evaluated.
628 Pseudotyping rabies with the VSV glycoprotein converts it into an anterograde tracer (Wickersham et al.,
629 2013). Combining injection of anterograde and retrograde rabies variants expressing different color fluorescent
630 proteins could simultaneously label the neurons projecting to that brain region and the axonal projections from
631 that brain region to its targets, providing an additional level of detail about relationships between neuronal
632 inputs and outputs. Rabies variants which express multiple transgenes in a single virus can be used to
633 simultaneously label different cellular compartments such as cytoplasmic GFP to visualize axonal arbors and
634 synaptophysin-RFP to label presynaptic profiles (Wickersham et al., 2013). This would allow for visualization of
635 rapid changes in synaptic connectivity during plasticity. These experiments could be specialized further by cell-
636 type specific infection.

637
638 Rabies virus pseudotyped with EnvA is a powerful intersectional approach which can be used to label neurons
639 in both an anatomically and genetically defined manner. As proof of principle, we expressed TVA in one tectal
640 lobe and then injected EnvA pseudotyped rabies into the other tectal lobe and successfully retrogradely
641 infected only intertectal neurons expressing TVA. In our system, VGAT promoter-driven expression of TVA is
642 biased toward inhibitory neurons but is not cell-type specific. This lack of specificity likely reflects cellular fate
643 specification in the developing tadpole brain. Neurons at the stages of development used in our study can
644 dynamically switch neurotransmitter expression (Borodinsky et al., 2004; Dulcis et al., 2013; Li et al., 2020).
645 Furthermore, the inhibitory neuron markers GABA and GAD67, and the excitatory neuron marker CaMKII, are
646 regulated by visual activity in the tadpole optic tectum (Miraucourt et al., 2012; Shen et al., 2014). In addition,
647 single cell RT-PCR showed that individual tectal neurons express transcripts of both excitatory and inhibitory
648 markers (Cline lab, unpublished observations). Nevertheless, cell-type specific expression plasmids, for
649 instance Sox2 in neural progenitor cells (Bestman et al., 2012), do function in the *Xenopus* brain. Therefore,
650 our results suggest that an intersectional strategy using cell-type specific expression of TVA is possible in
651 principle, based on the specificity of available promoters.

652
653 Driving TVA expression using cell-type specific promoters would permit the visualization of neurons triply-
654 defined by cell body location, genetics, and axon projection. Neuronal cell types are defined by a combination
655 of features including morphology, location, projection pattern, expression of genetic markers, and physiological
656 properties (Ecker et al., 2017). Describing cell types based on these features is essential to understanding their
657 function within the brain. The ability of rabies to label cells defined by a combination of features and
658 simultaneously drive expression of calcium indicators to visualize neuronal activity or optogenetic tools to
659 activate or deactivate them, can contribute a great deal to our understanding of neuronal cell types and their

660 functions (Osakada et al., 2011). In addition to EnvA/TVA, more flexibility in cell-type specific labeling is
661 possible using EnvB/TVB and EnvE/TVE pairs for targeting infection (Choi et al., 2010; Suzuki et al., 2019).
662 When these viruses drive expression of different color fluorescent proteins, they can be combined in a
663 multiplex strategy in which one performs retrograde infection of different Env(x) viruses from a single target
664 location and labels different genetically defined subpopulations of input neurons through specific TV(x)
665 expression. The versatility of these tools enables a variety of experiments to analyze and manipulate
666 mesoscale connectivity in *Xenopus*, a system that has contributed to understanding fundamental principles of
667 brain circuit development and plasticity, hormonal regulation of metamorphosis, and regeneration.

668

669

670 **References**

671

672 Aizenman CD, Cline HT (2007) Enhanced visual activity in vivo forms nascent synapses in the developing
673 retinotectal projection. *J Neurophysiol* 97:2949-2957.

674 Astic L, Saucier D, Coulon P, Lafay F, Flamand A (1993) The CVS strain of rabies virus as transneuronal
675 tracer in the olfactory system of mice. *Brain Res* 619:146-156.

676 Beier KT, Gao XJ, Xie S, DeLoach KE, Malenka RC, Luo L (2019) Topological Organization of Ventral
677 Tegmental Area Connectivity Revealed by Viral-Genetic Dissection of Input-Output Relations. *Cell Rep* 26:159-
678 167 e156.

679 Bestman JE, Ewald RC, Chiu SL, Cline HT (2006) In vivo single-cell electroporation for transfer of DNA and
680 macromolecules. *Nat Protoc* 1:1267-1272.

681 Bestman JE, Lee-Osbourne J, Cline HT (2012) In vivo time-lapse imaging of cell proliferation and
682 differentiation in the optic tectum of *Xenopus laevis* tadpoles. *J Comp Neurol* 520:401-433.

683 Borodinsky LN, Root CM, Cronin JA, Sann SB, Gu X, Spitzer NC (2004) Activity-dependent homeostatic
684 specification of transmitter expression in embryonic neurons. *Nature* 429:523-530.

685 Callaway EM (2008) Transneuronal circuit tracing with neurotropic viruses. *Curr Opin Neurobiol* 18:617-623.

686 Callaway EM, Luo L (2015) Monosynaptic Circuit Tracing with Glycoprotein-Deleted Rabies Viruses. *J*
687 *Neurosci* 35:8979-8985.

688 Chae J, Zimmerman LB, Grainger RM (2002) Inducible control of tissue-specific transgene expression in
689 *Xenopus tropicalis* transgenic lines. *Mech Dev* 117:235-241.

690 Choi J, Young JA, Callaway EM (2010) Selective viral vector transduction of ErbB4 expressing cortical
691 interneurons in vivo with a viral receptor-ligand bridge protein. *Proc Natl Acad Sci U S A* 107:16703-16708.

692 Conzelmann KK, Cox JH, Schneider LG, Thiel HJ (1990) Molecular cloning and complete nucleotide sequence
693 of the attenuated rabies virus SAD B19. *Virology* 175:485-499.

694 Dietzschold B (1977) Oligosaccharides of the glycoprotein of rabies virus. *J Virol* 23:286-293.

695 Dietzschold B, Li J, Faber M, Schnell M (2008) Concepts in the pathogenesis of rabies. *Future Virol* 3:481-490.

- 696 Dohaku R, Yamaguchi M, Yamamoto N, Shimizu T, Osakada F, Hibi M (2019) Tracing of Afferent Connections
697 in the Zebrafish Cerebellum Using Recombinant Rabies Virus. *Front Neural Circuits* 13:30.
- 698 Dulcis D, Jamshidi P, Leutgeb S, Spitzer NC (2013) Neurotransmitter switching in the adult brain regulates
699 behavior. *Science* 340:449-453.
- 700 Dutton JR, Daughters RS, Chen Y, O'Neill KE, Slack JM (2009) Use of adenovirus for ectopic gene expression
701 in *Xenopus*. *Dev Dyn* 238:1412-1421.
- 702 Ecker JR, Geschwind DH, Kriegstein AR, Ngai J, Osten P, Polioudakis D, Regev A, Sestan N, Wickersham IR,
703 Zeng H (2017) The BRAIN Initiative Cell Census Consortium: Lessons Learned toward Generating a
704 Comprehensive Brain Cell Atlas. *Neuron* 96:542-557.
- 705 Etesami R, Conzelmann KK, Fadai-Ghotbi B, Natelson B, Tsiang H, Ceccaldi PE (2000) Spread and
706 pathogenic characteristics of a G-deficient rabies virus recombinant: an in vitro and in vivo study. *J Gen Virol*
707 81:2147-2153.
- 708 Federspiel MJ, Bates P, Young JA, Varmus HE, Hughes SH (1994) A system for tissue-specific gene targeting:
709 transgenic mice susceptible to subgroup A avian leukosis virus-based retroviral vectors. *Proc Natl Acad Sci U*
710 *S A* 91:11241-11245.
- 711 Gambrill AC, Faulkner R, Cline HT (2016) Experience-dependent plasticity of excitatory and inhibitory
712 intertectal inputs in *Xenopus* tadpoles. *J Neurophysiol*:jn 00611 02016.
- 713 Gambrill AC, Faulkner RL, Cline HT (2018) Direct intertectal inputs are an integral component of the bilateral
714 sensorimotor circuit for behavior in *Xenopus* tadpoles. *J Neurophysiol* 119:1947-1961.
- 715 Haas K, Jensen K, Sin WC, Foa L, Cline HT (2002) Targeted electroporation in *Xenopus* tadpoles in vivo--from
716 single cells to the entire brain. *Differentiation* 70:148-154.
- 717 Haery L, Deverman BE, Matho KS, Cetin A, Woodard K, Cepko C, Guerin KI, Rego MA, Ersing I, Bachle SM,
718 Kamens J, Fan M (2019) Adeno-Associated Virus Technologies and Methods for Targeted Neuronal
719 Manipulation. *Front Neuroanat* 13:93.
- 720 Hafner G, Witte M, Guy J, Subhashini N, Fenno LE, Ramakrishnan C, Kim YS, Deisseroth K, Callaway EM,
721 Oberhuber M, Conzelmann KK, Staiger JF (2019) Mapping Brain-Wide Afferent Inputs of Parvalbumin-
722 Expressing GABAergic Neurons in Barrel Cortex Reveals Local and Long-Range Circuit Motifs. *Cell Rep*
723 28:3450-3461 e3458.
- 724 He HY, Shen W, Hiramoto M, Cline HT (2016) Experience-Dependent Bimodal Plasticity of Inhibitory Neurons
725 in Early Development. *Neuron* 90:1203-1214.
- 726 Hiramoto M, Cline HT (2009) Convergence of multisensory inputs in *Xenopus* tadpole tectum. *Dev Neurobiol*
727 69:959-971.
- 728 Hirsch N, Zimmerman LB, Grainger RM (2002) *Xenopus*, the next generation: *X. tropicalis* genetics and
729 genomics. *Dev Dyn* 225:422-433.
- 730 Kawakami Y, Rodriguez Esteban C, Raya M, Kawakami H, Marti M, Dubova I, Izpisua Belmonte JC (2006)
731 Wnt/beta-catenin signaling regulates vertebrate limb regeneration. *Genes Dev* 20:3232-3237.

732 Kelly RM, Strick PL (2000) Rabies as a transneuronal tracer of circuits in the central nervous system. *J*
733 *Neurosci Methods* 103:63-71.

734 Kim EJ, Jacobs MW, Ito-Cole T, Callaway EM (2016) Improved Monosynaptic Neural Circuit Tracing Using
735 Engineered Rabies Virus Glycoproteins. *Cell Rep* 15:692-699.

736 Lavin TK, Jin L, Lea NE, Wickersham IR (2020) Monosynaptic Tracing Success Depends Critically on Helper
737 Virus Concentrations. *Front Synaptic Neurosci* 12:6.

738 Li HQ, Pratelli M, Godavarthi S, Zambetti S, Spitzer NC (2020) Decoding Neurotransmitter Switching: The
739 Road Forward. *J Neurosci* 40:4078-4089.

740 Luo L, Callaway EM, Svoboda K (2018) Genetic Dissection of Neural Circuits: A Decade of Progress. *Neuron*
741 98:256-281.

742 Ma M, Kler S, Pan YA (2019) Structural Neural Connectivity Analysis in Zebrafish With Restricted Anterograde
743 Transneuronal Viral Labeling and Quantitative Brain Mapping. *Front Neural Circuits* 13:85.

744 Marshel JH, Mori T, Nielsen KJ, Callaway EM (2010) Targeting single neuronal networks for gene expression
745 and cell labeling in vivo. *Neuron* 67:562-574.

746 Mebatsion T, Konig M, Conzelmann KK (1996a) Budding of rabies virus particles in the absence of the spike
747 glycoprotein. *Cell* 84:941-951.

748 Mebatsion T, Schnell MJ, Cox JH, Finke S, Conzelmann KK (1996b) Highly stable expression of a foreign
749 gene from rabies virus vectors. *Proc Natl Acad Sci U S A* 93:7310-7314.

750 Miraucourt LS, Silva JS, Burgos K, Li J, Abe H, Ruthazer ES, Cline HT (2012) GABA expression and
751 regulation by sensory experience in the developing visual system. *PLoS One* 7:e29086.

752 Miyamichi K, Shlomai-Fuchs Y, Shu M, Weissbourd BC, Luo L, Mizrahi A (2013) Dissecting local circuits:
753 parvalbumin interneurons underlie broad feedback control of olfactory bulb output. *Neuron* 80:1232-1245.

754 Mundell NA, Beier KT, Pan YA, Lapan SW, Goz Ayturk D, Berezovskii VK, Wark AR, Drokhlyansky E, Bielecki
755 J, Born RT, Schier AF, Cepko CL (2015) Vesicular stomatitis virus enables gene transfer and transsynaptic
756 tracing in a wide range of organisms. *J Comp Neurol* 523:1639-1663.

757 Nassi JJ, Cepko CL, Born RT, Beier KT (2015) Neuroanatomy goes viral! *Front Neuroanat* 9:80.

758 Nieuwkoop PD, Faber J (1956). Normal table of *Xenopus laevis* (Daudin); a systematical and chronological
759 survey of the development from the fertilized egg till the end of metamorphosis. Amsterdam,; North-Holland
760 Pub. Co.

761 Osakada F, Mori T, Cetin AH, Marshel JH, Virgen B, Callaway EM (2011) New rabies virus variants for
762 monitoring and manipulating activity and gene expression in defined neural circuits. *Neuron* 71:617-631.

763 Parr-Brownlie LC, Bosch-Bouju C, Schoderboeck L, Sizemore RJ, Abraham WC, Hughes SM (2015) Lentiviral
764 vectors as tools to understand central nervous system biology in mammalian model organisms. *Front Mol*
765 *Neurosci* 8:14.

- 766 Reardon TR, Murray AJ, Turi GF, Wirblich C, Croce KR, Schnell MJ, Jessell TM, Losonczy A (2016) Rabies
767 Virus CVS-N2c(DeltaG) Strain Enhances Retrograde Synaptic Transfer and Neuronal Viability. *Neuron* 89:711-
768 724.
- 769 Ruthazer ES, Li J, Cline HT (2006) Stabilization of axon branch dynamics by synaptic maturation. *J Neurosci*
770 26:3594-3603.
- 771 Schnell MJ, McGettigan JP, Wirblich C, Papaneri A (2010) The cell biology of rabies virus: using stealth to
772 reach the brain. *Nat Rev Microbiol* 8:51-61.
- 773 Session AM, et al. (2016) Genome evolution in the allotetraploid frog *Xenopus laevis*. *Nature* 538:336-343.
- 774 Shakin-Eshleman SH, Remaley AT, Eshleman JR, Wunner WH, Spitalnik SL (1992) N-linked glycosylation of
775 rabies virus glycoprotein. Individual sequons differ in their glycosylation efficiencies and influence on cell
776 surface expression. *J Biol Chem* 267:10690-10698.
- 777 Shen W, Liu HH, Schiapparelli L, McClatchy D, He HY, Yates JR, 3rd, Cline HT (2014) Acute synthesis of
778 CPEB is required for plasticity of visual avoidance behavior in *Xenopus*. *Cell Rep* 6:737-747.
- 779 Sin WC, Haas K, Ruthazer ES, Cline HT (2002) Dendrite growth increased by visual activity requires NMDA
780 receptor and Rho GTPases. *Nature* 419:475-480.
- 781 Stepien AE, Tripodi M, Arber S (2010) Monosynaptic rabies virus reveals premotor network organization and
782 synaptic specificity of cholinergic partition cells. *Neuron* 68:456-472.
- 783 Suzuki T, Morimoto N, Akaike A, Osakada F (2019) Multiplex Neural Circuit Tracing With G-Deleted Rabies
784 Viral Vectors. *Front Neural Circuits* 13:77.
- 785 Thoulouze MI, Lafage M, Schachner M, Hartmann U, Cremer H, Lafon M (1998) The neural cell adhesion
786 molecule is a receptor for rabies virus. *J Virol* 72:7181-7190.
- 787 Tuffereau C, Benejean J, Blondel D, Kieffer B, Flamand A (1998) Low-affinity nerve-growth factor receptor
788 (P75NTR) can serve as a receptor for rabies virus. *EMBO J* 17:7250-7259.
- 789 Tuffereau C, Schmidt K, Langevin C, Lafay F, Dechant G, Koltzenburg M (2007) The rabies virus glycoprotein
790 receptor p75NTR is not essential for rabies virus infection. *J Virol* 81:13622-13630.
- 791 Ugolini G (1995) Specificity of rabies virus as a transneuronal tracer of motor networks: transfer from
792 hypoglossal motoneurons to connected second-order and higher order central nervous system cell groups. *J*
793 *Comp Neurol* 356:457-480.
- 794 Ugolini G (2010) Advances in viral transneuronal tracing. *J Neurosci Methods* 194:2-20.
- 795 Vercelli A, Repici M, Garbossa D, Grimaldi A (2000) Recent techniques for tracing pathways in the central
796 nervous system of developing and adult mammals. *Brain Res Bull* 51:11-28.
- 797 Wall NR, Wickersham IR, Cetin A, De La Parra M, Callaway EM (2010) Monosynaptic circuit tracing in vivo
798 through Cre-dependent targeting and complementation of modified rabies virus. *Proc Natl Acad Sci U S A*
799 107:21848-21853.
- 800 Wang J, Wang Z, Liu R, Shuai L, Wang X, Luo J, Wang C, Chen W, Wang X, Ge J, He X, Wen Z, Bu Z (2018)
801 Metabotropic glutamate receptor subtype 2 is a cellular receptor for rabies virus. *PLoS Pathog* 14:e1007189.

- 802 Wickersham IR, Finke S, Conzelmann KK, Callaway EM (2007a) Retrograde neuronal tracing with a deletion-
803 mutant rabies virus. *Nat Methods* 4:47-49.
- 804 Wickersham IR, Lyon DC, Barnard RJ, Mori T, Finke S, Conzelmann KK, Young JA, Callaway EM (2007b)
805 Monosynaptic restriction of transsynaptic tracing from single, genetically targeted neurons. *Neuron* 53:639-647.
- 806 Wickersham IR, Sullivan HA, Seung HS (2010) Production of glycoprotein-deleted rabies viruses for
807 monosynaptic tracing and high-level gene expression in neurons. *Nat Protoc* 5:595-606.
- 808 Wickersham IR, Sullivan HA, Seung HS (2013) Axonal and subcellular labelling using modified rabies viral
809 vectors. *Nat Commun* 4:2332.
- 810 Wirblich C, Schnell MJ (2011) Rabies virus (RV) glycoprotein expression levels are not critical for pathogenicity
811 of RV. *J Virol* 85:697-704.
- 812 Wu GY, Zou DJ, Koothan T, Cline HT (1995) Infection of frog neurons with vaccinia virus permits in vivo
813 expression of foreign proteins. *Neuron* 14:681-684.
- 814 Wunner WH, Curtis PJ, Wiktor TJ (1980) Rabies mRNA translation in *Xenopus laevis* oocytes. *J Virol* 36:133-
815 142.
- 816 Yamaguchi A, Woller DJ, Rodrigues P (2018) Development of an Acute Method to Deliver Transgenes Into the
817 Brains of Adult *Xenopus laevis*. *Front Neural Circuits* 12:92.
- 818 Yan X, Mohankumar PS, Dietzschold B, Schnell MJ, Fu ZF (2002) The rabies virus glycoprotein determines
819 the distribution of different rabies virus strains in the brain. *J Neurovirol* 8:345-352.
- 820 Young JA, Bates P, Varmus HE (1993) Isolation of a chicken gene that confers susceptibility to infection by
821 subgroup A avian leukosis and sarcoma viruses. *J Virol* 67:1811-1816.
- 822 Zeng H (2018) Mesoscale connectomics. *Curr Opin Neurobiol* 50:154-162.
- 823 Zhu P, Narita Y, Bundschuh ST, Fajardo O, Scharer YP, Chattopadhyaya B, Bouldoires EA, Stepien AE,
824 Deisseroth K, Arber S, Sprengel R, Rijli FM, Friedrich RW (2009) Optogenetic Dissection of Neuronal Circuits
825 in Zebrafish using Viral Gene Transfer and the Tet System. *Front Neural Circuits* 3:21.
- 826 Zhu X, Lin K, Liu Q, Yue X, Mi H, Huang X, He X, Wu R, Zheng D, Wei D, Jia L, Wang W, Manyande A, Wang
827 J, Zhang Z, Xu F (2020) Rabies Virus Pseudotyped with CVS-N2C Glycoprotein as a Powerful Tool for
828 Retrograde Neuronal Network Tracing. *Neurosci Bull* 36:202-216.

829

830 **Tables**

831

832 Table 1: Statistical Table

833

	Data structure	Type of test	p-value	Sample size (n=tadpoles)
a		Fisher's exact test	0.37	22°C n=12 28°C n=11
b		Fisher's exact test	0.63	CMV::gal4 n=4 VGAT::gal4 n=21
c	Not normally distributed	Mann-Whitney U test	<0.0001	gal4-UAS amplification n=9 No gal4-UAS amplification n=14
d	Not normally distributed	Mann-Whitney U test	0.74	B19G ⁺ n=17 B19G ⁻ n=11

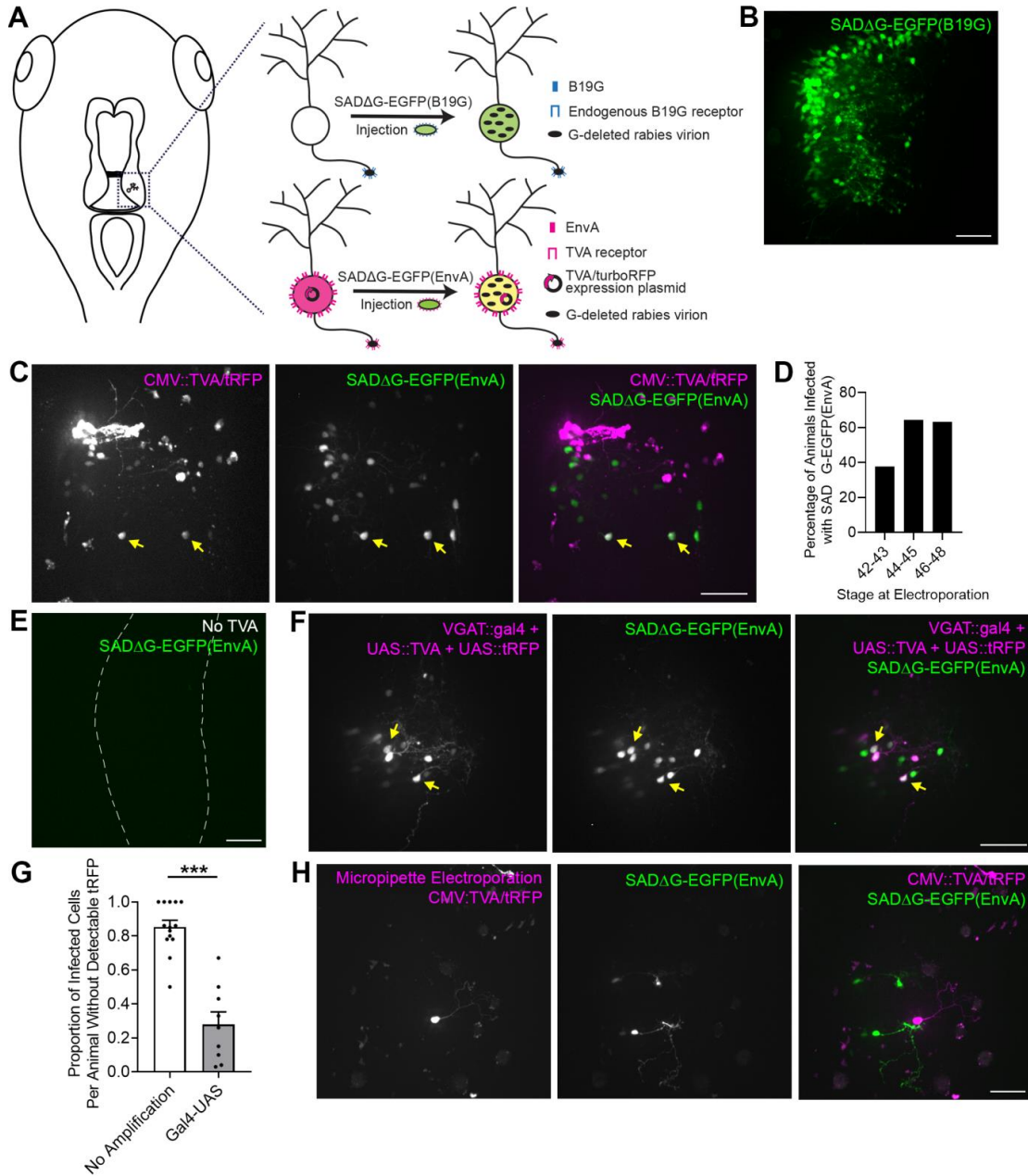
834

835 For each statistical test run in the study, the data structure, statistical test, p-value, and sample size are listed.

836

837
838
839

Figures



840
841
842

Figure 1. Pseudotyped recombinant rabies virus infects tectal neurons in the *Xenopus* tadpole.

843 **A.** Schematic of the labeling strategies using recombinant SAD B19 rabies virus which has the glycoprotein
844 deleted and replaced by EGFP (SADΔG-EGFP), rendering it incapable of transneuronal spread. Infection with
845 B19G phenotypically complemented virus (top) relies on endogenous expression of the B19G receptor.
846 Infection with EnvA pseudotyped virus (bottom) requires exogenous expression of its receptor, TVA, prior to
847 viral injection. Co-labeling TVA-transfected neurons with turboRFP (tRFP) allows them to be identified. Viral
848 injections were made in the optic tectum, which is marked by a dashed box in the drawing to the left.

849 **B.** SADΔG-EGFP(B19G) virus infects tectal neurons. Confocal Z-projection collected in vivo through the
850 injected optic tectal lobe shows widespread virally-mediated expression of EGFP in infected neurons.

851 **C.** SADΔG-EGFP(EnvA) virus infects tectal neurons transfected with TVA. The right optic tectal lobe was
852 transfected with CMV::TVA/tRFP by whole-brain electroporation and injected with SADΔG-EGFP(EnvA) virus 4
853 days later. Confocal Z-projections collected in vivo through the optic tectal lobe electroporated with
854 CMV::TVA/tRFP (magenta) and injected with SADΔG-EGFP(EnvA) virus (green). Neurons which co-express
855 TVA/tRFP and viral EGFP are marked by yellow arrows. The remaining EGFP-expressing neurons lack
856 detectable tRFP expression and are presumably invisible TVA-expressing neurons.

857 **D.** Viral infection efficiency varies with developmental stage. Tadpoles at stages 42-43 (n=16 tadpoles), 44-45
858 (n=28 tadpoles), or 46-48 (n=65 tadpoles) were electroporated with CMV::TVA/tRFP using whole-brain
859 electroporation. Four days later, the transfected tectal lobe was injected with SADΔG-EGFP(EnvA) virus. The
860 percentage of animals with EGFP-expressing neurons was highest between stages 44-48.

861 **E.** Infection with SADΔG-EGFP(EnvA) virus requires TVA. Confocal Z-projection collected in vivo through an
862 optic tectal lobe injected with SADΔG-EGFP(EnvA) shows no infected neurons in the absence of TVA
863 electroporation.

864 **F.** SADΔG-EGFP(EnvA) infects tectal neurons transfected with TVA driven by the VGAT promoter. The right
865 optic tectal lobe was transfected with VGAT::gal4, UAS::TVA, and UAS::tRFP by whole-brain electroporation
866 and injected with SADΔG-EGFP(EnvA) virus 4 days later. Confocal Z-projections collected in vivo through the
867 optic tectal lobe showing electroporated (magenta) and infected (green) tectal neurons. Neurons which co-
868 express TVA/tRFP and viral EGFP are marked by yellow arrows. The remaining EGFP-expressing neurons
869 lack detectable tRFP expression and are invisible TVA-expressing neurons.

870 **G.** Quantification of the proportion of invisible TVA cells per animal with and without amplification. Amplifying
871 tRFP expression using the gal4-UAS system decreases the proportion of infected, EGFP⁺ cells that lack
872 detectable tRFP compared to tRFP driven by the CMV promoter without amplification. Data are presented as
873 mean ± SEM overlaid with individual data points (p<0.0001, Mann-Whitney test).

874 **H.** Targeted electroporation of TVA/tRFP does not eliminate invisible TVA-expressing neurons. Micropipette-
875 mediated electroporation was used to limit transfection with TVA/tRFP to one or few neurons in the right optic
876 tectal lobe. Four days later, the electroporated tectal lobe was injected with SADΔG-EGFP(EnvA) virus.
877 Confocal Z-projection collected in vivo through the optic tectal lobe shows that EGFP-expressing infected
878 neurons which lack detectable tRFP are still present.

879 Scale bars=50 μ m.

880

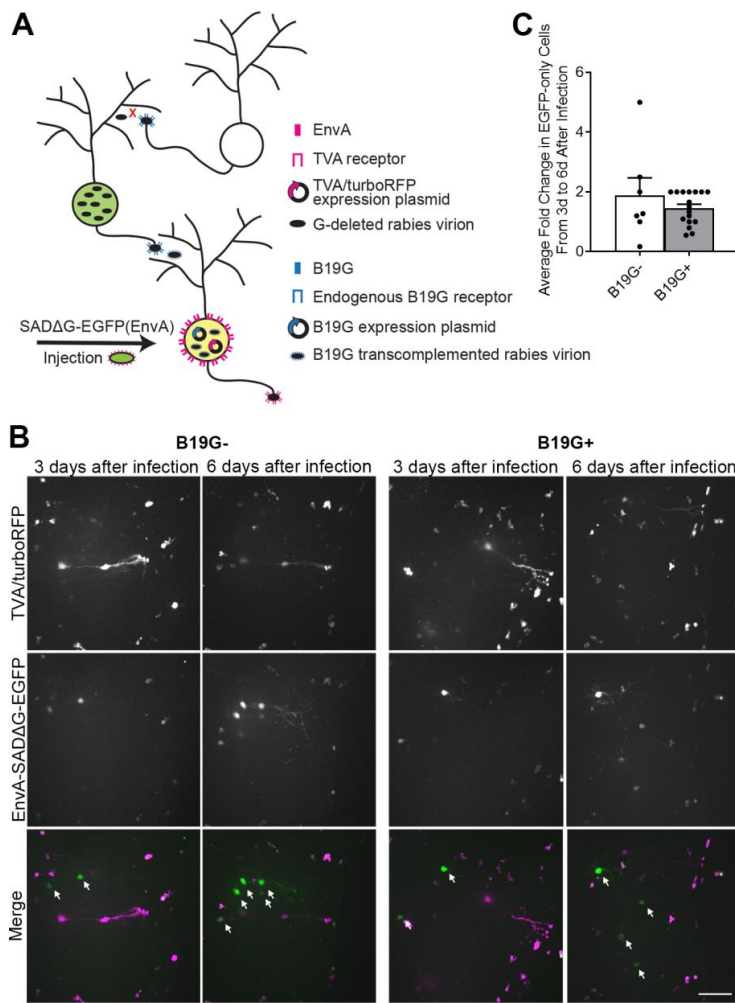


Figure 2. Transcomplementation with rabies glycoprotein does not result in transneuronal spread of recombinant rabies in tadpoles.

A. Schematic of the monosynaptic tracing strategy using SADΔG-EGFP(EnvA) virus with transcomplementation of rabies glycoprotein, B19G. Neurons co-transfected with TVA/tRFP and B19G can be directly infected by EnvA pseudotyped virus through the TVA receptor. Viral particles which bud from directly infected neurons will have B19G on their surface because B19G is provided in *trans*. In mammals, those viral particles can infect presynaptic neurons through the endogenous B19G receptor. Because presynaptically infected neurons lack B19G expression, viral particles generated in those neurons lack the glycoprotein and are not infectious, thereby prohibiting further spread.

B. In vivo time-lapse imaging of infected tectal neurons from 3-6d following injection of SADΔG-EGFP(EnvA) virus in the presence or absence of B19G. One tectal lobe was transfected with TVA/tRFP (magenta) alone

894 (left) or with TVA/tRFP and B19G (right) and then injected with SADΔG-EGFP(EnvA) virus 4 days later. At 3
895 and 6 days after viral injection, confocal Z-stacks through the tectal lobe were collected. Z-projections show an
896 increase in the number of EGFP⁺ neurons without detectable tRFP (white arrows) from 3-6 days after viral
897 injection in both the presence and absence of B19G. Scale bar=50μm.

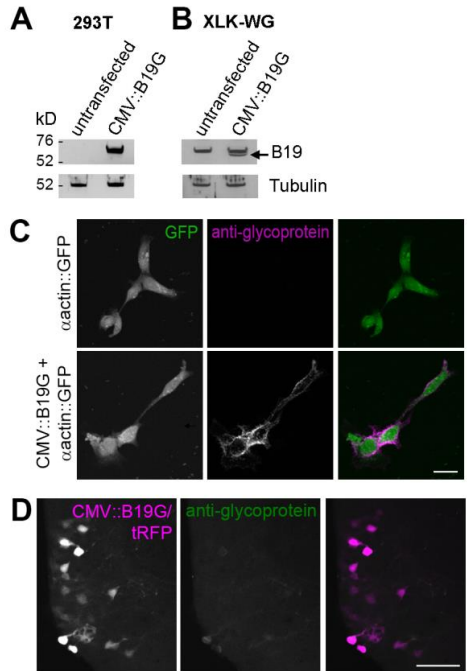
898 **C.** Quantification of the average fold-change in the number of EGFP-only cells from 3-6 day after injection.

899 There is a similar increase in the average number of EGFP-only cells over time in the presence (n=17
900 tadpoles) and absence (n=7 tadpoles) of B19G, suggesting a lack of local presynaptic spread of rabies virus.

901 Data are presented as mean ± SEM overlaid with individual data points (p=0.74, Mann-Whitney U test).

902

903



904

905

906 **Figure 3. Weak expression of B19G in vivo may explain the lack of transneuronal spread of rabies**
 907 **virus.**

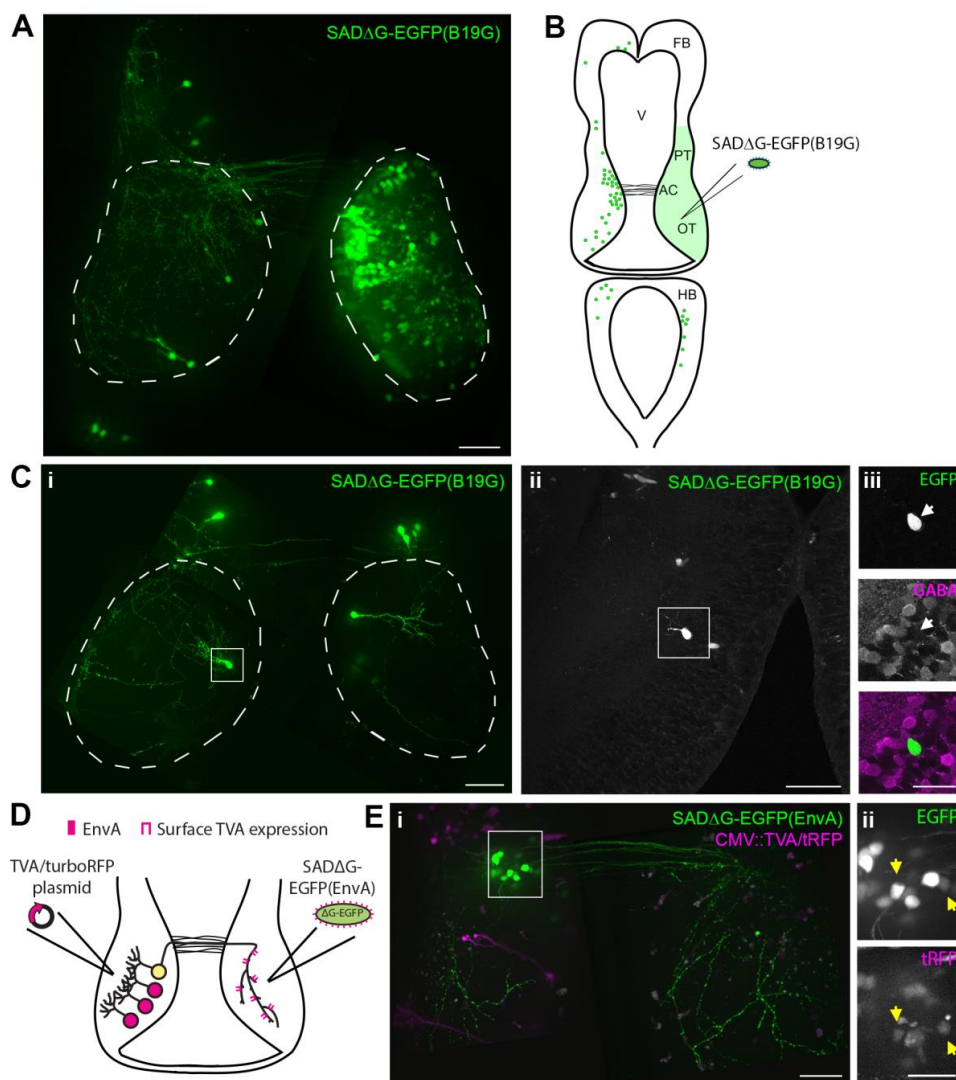
908

909 **A,B.** Rabies glycoprotein is detected in the membrane fraction of transfected mammalian and Xenopus cell
 910 cultures by western blot. 293T (**A**) and XLK-WG Xenopus kidney cells (**B**) were transfected with B19G and
 911 proteins were extracted 24 hours later. Membrane fractions were probed for B19G expression with anti-rabies
 912 glycoprotein antibody and β -tubulin acted as a loading control. Compared to untransfected cells, specific bands
 913 of approximately 70kD were visible in transfected cells. Specific band in transfected XLK-WG cells is denoted
 914 by an arrow (**B**). kD: kilodaltons.

915 **C.** Rabies glycoprotein is detected on the surface of Xenopus cells in vitro by immunocytochemistry. XLK-WG
 916 cells were transfected with GFP alone (top) or B19G and GFP (bottom). Confocal Z-projections of cells
 917 transfected with both B19G and GFP show surface expression of B19G by anti-rabies glycoprotein
 918 immunocytochemistry (magenta) without permeabilization. In contrast, no anti-rabies glycoprotein
 919 immunoreactivity is observed in cells transfected with GFP alone. Scale bar=20 μ m.

920 **D.** Expression of B19G is very weak in vivo in tectal neurons. Tectal neurons were electroporated with
 921 CMV::B19G/tRFP, fixed 3-4 days later, and then immunohistochemistry with anti-rabies glycoprotein was

922 performed. Confocal Z-projection of a 40um tissue slice shows very weak immunoreactivity for rabies
 923 glycoprotein (green) in B19G/tRFP expressing neurons (magenta). Scale bar=50µm.
 924



925
 926
 927
 928
 929
 930
 931
 932

Figure 4. Retrograde neuronal tracing using recombinant rabies virus.

A. SADΔG-EGFP(B19G) virus retrogradely labels afferents to the injected target region. A montage of confocal Z-projections collected in vivo shows neurons infected by injection of SADΔG-EGFP(B19G) virus into the right tectal lobe. In addition to a large number of neurons expressing EGFP in the injected tectal lobe, retrogradely infected projection neurons are visible in the contralateral tectum, pretegmentum, and hindbrain. Tectal lobes are marked with dashed lines. Scale bar=50µm.

933 **B.** A schematic which maps neurons labeled by unilateral tectal injection of SADΔG-EGFP(B19G) virus.
934 Neurons in several regions known to project to the optic tectum are labeled. We also observed a large number
935 of neurons in the injected tectal lobe and ipsilateral pretectum (green shading). AC: anterior commissure, FB:
936 forebrain, HB: hindbrain, OT: optic tectum, PT: pretectum, V: ventricle.

937 **C.** Retrograde viral tracing paired with immunohistochemistry reveals the cell-types which project between the
938 two tectal lobes. A montage of confocal Z-projections collected in vivo following injection of SADΔG-
939 EGFP(B19G) virus into the right tectal lobe shows retrograde tracing of one intertectal neuron (boxed in left
940 tectal lobe) (i). Following fixation and tissue sectioning, immunohistochemistry was performed with an anti-
941 GABA antibody to label inhibitory neurons. The EGFP⁺ neuron imaged in vivo (i) could be identified in fixed
942 tissue slice (ii) and was GABA-negative (iii, magenta), suggesting that it is excitatory. Scale bars=50μm (i, ii)
943 and 25μm (iii).

944 **D.** Schematic showing retrograde tracing strategy used in **E**. The left tectal lobe is electroporated with
945 TVA/tRFP and 4 days later, SADΔG-EGFP(EnvA) virus is injected into the right tectal lobe. Expression of TVA
946 on the surface of intertectal axons mediates viral infection of intertectal neurons in the left hemisphere.

947 **E.** SADΔG-EGFP(EnvA) virus can be used to retrogradely trace neurons defined by anatomical location and
948 axonal projections using promoter-driven expression of TVA. A montage of confocal Z-projections collected in
949 vivo (i) demonstrate retrograde tracing of TVA-expressing neurons in the left tectal lobe (magenta) following
950 injection of SADΔG-EGFP(EnvA) virus into the right tectal lobe. Retrogradely infected neurons (boxed in i) are
951 shown at higher magnification (ii) and cells co-expressing EGFP and tRFP are marked by yellow arrows. Scale
952 bars=50μm (i) and 25μm (ii).

